Revista Mexicana de Astronomía y Astrofísica, **60**, 69–81 (2024)

https://doi.org/10.22201/ia.01851101p.2024.60.01.05

INVESTIGATION ON FOUR CONTACT BINARY SYSTEMS AND A SEMI-DETACHED ONE AT THE BEGINNING OF THE CONTACT PHASE

F. Acerbi[1], M. Martignoni[1], R. Michel[2], C. Barani[1], H. Aceves[2], L. Altamirano-Dévora[2], and F. J. Tamayo[3]

Received July 3 2023; accepted September 25 2023

ABSTRACT

We present B, V, R_c and I_c light curves of four contact binary systems and one semi-detached system. New observations confirm and revise the short-period (0.22–0.25d) of the systems and that all stars belong to the spectral type K. In J105924 and J164349 a third light was found while the shape of the light curves of four systems (excluding J105924) suggests the presence of inhomogeneities on the surface of one component which confirms that the systems are active. Also they are observed at low orbital inclination $i \in (41^o, 62^o)$. The temperature difference range is $\Delta T \in (4, 640)$K and the mass ratios $q \in (0.20, 0.75)$. Absolute parameters are estimated using statistical diagrams. The systems follow the general pattern of the relative subtype of W Ursae Majoris systems. The sum of the component masses of four systems is below the mass limit of $1.0 - 1.2 M_\odot$ assumed for the known contact binary stars; this tells us that they belong to the class of low mass contact binaries.

RESUMEN

Se presentan curvas de luz en B, V, R_c e I_c de cuatro binarias en contacto y un sistema semi-ligado. Nuevas observaciones confirman y actualizan los cortos períodos (0.22-0.25d) de los sistemas y que todas las estrellas son del tipo espectral K. En J105924 y J164349 se encontró una tercera luz, mientras que en cuatro sistemas (excluyendo J105924) se sugiere la presencia de inhomogeneidad en la superficie de un componente, confirmando que los sistemas están activos. También tienen una inclinación orbital baja $i \in (41^o, 62^o)$, diferencias en temperatura $\Delta T \in (4, 640)$K, y cocientes de masa $q \in (0.20, 0.75)$. Los parámetros absolutos se estiman utilizando diagramas estadísticos. Los sistemas siguen el patrón general del subtipo W Ursae Majoris. La suma de las masas en cuatro sistemas está por debajo del límite de masa de 1.0–1.2$M_\odot$, asumido para las estrellas binarias de contacto conocidas; esto nos dice que pertenecen a la clase de binarias de contacto de baja masa.

Key Words: stars: individual: 1SWASP J105924.30+220458.0, 1SWASP J123609.78+341159.5, 1SWASP J161858.05+261303.5 (V1458 Her), 1SWASP J164349.61+325637.8 (V1475 Her), 1SWASP J132308.74+424613.3 (HW CVn) — techniques: photometric

1. INTRODUCTION

Our knowledge of binary systems allows us to divide them in three large groups. (1) The detached systems, in which both the stars are inside their respective Roche lobes without interactions between the components. (2) The semi-detached systems, with mass transfer from a component that fills its Roche lobe to the other one. And (3) contact, or over-contact, binaries that share the same outer atmosphere, the common convective envelope (CCE), and generally are in thermal and physical contact.

The transition between semidetached to contact phase, and viceversa, is predicted by the thermal relaxation oscillation theory (TRO theory) (Lucy 1976; Flannery 1976; Robertson & Eggleton 1977; Yakut & Eggleton 2005; Li et al. 2008). TRO considers that the mass transfer between the components causes them to evolve oscillating in a cycle, where the flow of mass is reversed and the contact binary evolves

[1]Stazione Astronomica Betelgeuse, Magnago, Italy.
[2]Instituto de Astronomía, UNAM. Ensenada, México.
[3]Facultad de Ciencias Físico-Matemáticas, UANL, Nuevo León, México.

TABLE 1

PARAMETERS OF THE TARGETS FROM THE VSX DATABASE

Target	RA(2000)	Dec(2000)	Period, d	Ampl.	Reference
J105924	10 59 24.30	+22.04.58.5	0.231092	0.12	Drake et al. (2014)
J123609	12 36 09.75	+34.11.59.7	0.248408	0.19	Drake et al. (2014)
J132308	13 23 08.74	+42 46 13.0	0.225133	0.16	Butters et al.(2010)
J161858	16 18 57.85	+26 13 38.5	0.228779	0.17	Butters et al.(2010)
J164349	16 43 49.61	+32 56 37.8	0.2250909	0.11	Akerlof et al. (2000)

toward small mass ratios q. Upon reaching the q_{min} the contact binary becomes unstable and may coalesce as progenitor of a single rapidly rotating star (Stępień (2011); Tylenda et al. (2011); Zhu et al. (2016); Liao et al. (2017); Li et al. (2021); Li et al. (2022) .

All the systems analyzed in this work belong to the spectral type K. The contact K-type systems here presented are of particular interest because only a few of them are well studied, especially systems with periods shorter than 0.25 days that are important objects for explaining the period cut-off phenomenon (Paczyński et al. (2006); Ruciński & Pribulla (2008); Liu et al. (2014); Li et al. (2019)).

It is clear that the study of binary systems is fundamental to acquire information about their formation and evolutionary status. The objective of this work is to acquire and estimate properties of a set of CBs using high quality photometric data and empirical relations.

2. INFORMATION ABOUT THE SYSTEMS

1SWASP J105924.30+220458.0 (J105924) and 1SWASP J123609.78+341159.5 (J123609) were found to be variable stars in the region covered by the Catalina Surveys Data Release-1 (CSDR1) (Drake et al. 2014). The type of variation was given for both systems (W UMa type), the amplitude as 0.12 mag. and the period as 0.231092 days for J105924; and the amplitude as 0.19 mag. and the period as 0.248408 days for J123609.

1SWASP J132308.74+424613.3 (J132308 = HW CVn): the type of variability was reported by Butters et al. (2010) as a generical EA/EB in the first WASP public data release. The period was identified by Lohr et al. (2013) as 19451.249s or 0.225130 days while the 5^{th} edition of the General Catalogue of Variable Stars (GCVS) by Samus' et al. (2017) report the first complete ephemerides:

$$HJD = 2456311.0270 + 0.225133\,E. \qquad (1)$$

The type of variability is EW and the amplitude of the light variation is 0.35 mag.

The first period for 1SWASP J161858.05 +261303.5 (J161858 = V1458 Her) was found by Lohr et al. (2013) as 19766.679s or 0.228781 days, and Samus' et al. (2017) in the GCVS report the complete ephemeris

$$HJD = 2456395.9480 + 0.228779\,E. \qquad (2)$$

suggesting the type of variation and a low amplitude of 0.17 mag. The system was analysed in a 2020 article (Li et al. 2020) together with other eight contact binaries around the short-period cutoff; a comparison of the results will be discussed later.

1SWASP J164349.61+325637.8 (J164349 = V1475 Her) was first reported as a Delta Scuti star in the Robotic Optical Transient Search Experiment I (ROTSE-I) surveys (Akerlof et al. 2000) with the half period of 0.11255 days. The correct period (19447.858s or 0.225091 days) and the nature of the eclipsing system was reported again by Lohr et al. (2013). The complete ephemerides was published in the GCVS (Samus' et al. 2017):

$$HJD = 2456459.8550 + 0.225091\,E. \qquad (3)$$

The amplitude of the EW light variation was found to be 0.21 mag.

J123609 and J164349, with a mass ratio $q > 0.72$ are considered high mass ratio systems, or H-type systems, as suggested by Csizmadia & Klagyivik (2004).

3. OBSERVATIONS AND NEW EPHEMERIDES

The preliminary available information about the targets was taken from the AAVSO Variable Star Index database (VSX) and is presented in Table 1.

All the observations were carried out at the San Pedro Mártir National Observatory (SPM, México) with the 0.84-m telescope (an f/15 Ritchey-Chretien), the Mexman filter-wheel and the *Marconi 5* CCD detector (an e2v CCD231-42 chip with $15 \times 15\mu^2$ pixels, gain of 2.38 e^-/ADU and readout noise of 4.02 e^-). The field of view was $9' \times 9'$

TABLE 2

LOG OF THE OBSERVATIONS

Object	UTObsDate	Hours	ExpTime B	ExpTime V	ExpTime R	ExpTime I
J105924	2022-03-27	5.75	40	20	15	15
J123609	2022-03-26	7.53	40	20	15	15
	2022-04-27	2.63	80	40	30	30
	2023-03-29	6.54	60	40	25	25
J132308	2022-03-23	5.47	40	20	15	15
	2022-03-25	1.88	40	20	15	15
J161858	2022-04-23	4.44	-	40	20	15
	2022-04-25	5.71	40	20	15	15
J164349	2022-04-14	5.81	40	20	15	15

TABLE 3

TIMES OF MINIMUM AND NEW EPHEMERIDES FROM OUR OBSERVATIONS

Object	HJD	Epoch	O-C	Error	Source	New Ephemerides	
J105924	2459665.6977	-0.5	0	0.0027	[1]	HJD 2459665.8122(10)	0.d2290620(5)
	2459665.8122	0	0	0.0032	[1]		
J123609	2459664.7260	0	0.0002	0.0057	[1]	HJD 2459664.7258(11)	0.d2484199(171)
	2459664.8480	0.5	-0.002	0.0047	[1]		
	2459664.9760	1	0.0018	0.0044	[1]		
	2459696.6477	128.5	0	0.0028	[1]		
J132308	2456311.0270	0	0	-	[2]	HJD 2456311.0270(14)	0.d2251345(1)
	2459661.8169	14883.5	0.001	0.0016	[1]		
	2459663.9537	14893	-0.001	0.002	[1]		
J161858	2456395.9480	0	0	-	[2]	HJD 2456395.9480(20)	0.d2287771(2)
	2459694.8008	14419.5	0.0014	0.0024	[1]		
	2459694.9124	14420	-0.0014	0.0019	[1]		
J164349	2456459.8550	0	0	-	[2]	HJD 2456459.8550(13)	0.d2250909(1)
	2459683.8340	14323	0.0014	0.0016	[1]		
	2459683.9439	14323.5	-0.0012	0.0018	[1]		
	2459711.8561	14447.5	-0.0002	0.0018	[1]		

[1] This paper. [2] AAVSO VSX.

and a binning of 2×2 was employed during all the observations.

Alternated exposures in filters B, V, R_c and I_c were taken during the observing runs. The details of the observations are shown in Table 2.

All the images were processed using IRAF[4] routines. Images were bias subtracted and flat field corrected before the instrumental magnitudes were computed with the standard aperture photometry method.

[4]IRAF is distributed by the National Optical Observatories, operated by the Association of Universities for Research in Astronomy, Inc., under cooperative agreement with the National Science Foundation.

In Table 3 are reported the ToMs and the new ephemerides derived from our observations.

The Transiting Exoplanet Survey Satellite (TESS; Prša et al. (2022)) provides some photometric data for our binary systems expressed in what are called T-magnitudes. These magnitudes are derived under some assumptions from the properties of the binary stars and their magnitudes at different wavelengths (Stassun et al. 2018). Here we abstain from using T-magnitude data and prefer to use our four clear-cut photometric bands data from SPM, and leave for future work a possible comparison on how the derived parameters here are affected when using the TESS data. Given the excellent quality and multi-wavelength data of our terrestrial obser-

TABLE 4

TARGET TEMPERATURE

Target	[1]	[2]	[3]	[4]	[5]	[6]	[7]	[8]	[9]	[10]
J105924	5022									5022
J123609		4996	4890	4890	4731	4844	4814			4860
J132308			4447	4447	4377	4638	4452		4542	4480
J161858				4580						4580
J164349			4457	4324				4361		4380

[1] LAMOST DR7, (Qian et al. 2020), [2] CRTS VSC, (Marsh et al. 2017), [3] ATLAS Refecat2, (Tonry et al. 2018), [4] Gaia DR2, (Brown et al. 2018), [5] Regression in GaiaDR2, (Bai et al. 2019), [6] Gaia EDR3, (Anders et al. 2022), [7] TESS Input Catalog - v8.0, (Stassun et al. 2019), [8] TESS Input Catalog - v8.2, (Paegert et al. 2021), [9] SDSS, (Miller 2015), [10] Average.

vations we conjecture that differences might be in the last one or two digits of our derived values reported below.

4. PHOTOMETRIC SOLUTION WITH THE W-D METHOD

The light curves of the systems were analyzed using the latest version of the Wilson-Devinney (W-D) code (Wilson & Devinney (1971); Wilson (1990); Wilson & van Hamme. (2016)).

Before starting the analysis some input parameters must be fixed, one of the most important being the temperature of the primary component (T_1). For this purpose, we have averaged the temperatures published in different stellar surveys (Table 4) and used this value in our set of parameters.

The temperature of the primary component of the systems suggests a convective envelope. Hence, we fixed in the W-D code the following atmospheric parameters to their theoretical values: the gravity-darkening coefficients $g_1 = g_2 = 0.32$ (Lucy 1967) and the bolometric albedos $A_1 = A_2 = 0.5$ (Ruciński 1973); the limb-darkening values originate from van Hamme (1993) for $\log g = 4.0$ and solar abundances.

The other parameters left as adjustable during the calculation were those suggested by the operation Mode 3 of the code; Mode 3 is used for the analysis of binary systems in contact and the free parameters are the orbital inclination i, the mean surface effective temperature of the secondary component T_2, the dimensionless surface potentials of the primary and secondary stars $\Omega_1 = \Omega_2$, the monochromatic luminosity of the primary component L_1 and the third light L_3.

The well-known q-search method was used to find the best initial mass ratio value fixed at each iteration and increased by 0.05 from $q = 0.05$ to 1 and by 0.1 beyond $q = 1$, since the mean residual showed a minimum.

For the systems J105924 and J164349, the results indicated the presence of a third light while for the other three systems the values for third light were negligible (smaller than the uncertainties).

The well know O'Connell effect, i.e. the different height of the maxima, (O'Connell 1951) is visible in the light curves of four of the systems (Figure 2). For this reason the spot parameters, co-latitude θ, longitude ϕ, angular radius γ, and the temperature factor T_s/T_* were treated as free.

For system J132308 we were not able to find a good fit to its light curves using Mode 3, so we switched to Mode 2, a detached configuration with no constraint on the potentials (Leung & Wilson 1977) to test the semi-detached configuration. After few iterations, the solution converged to Mode 5 – a semi-detached configuration with star 2 filling its Roche lobe. Using this Mode, the fixed parameters are the same of Mode 3 while among the free parameters Ω_1 is adjustable and Ω_2 is fixed by the code to the respective value of the mass ratio, so that the secondary component accurately fills its Roche lobe.

In Figure 1 the behavior of the q search procedure is visible, where the mean residual for the input data (Σ) is plotted against the value of the mass ratio q.

The value of q corresponding to the minimum value of Σ was subsequently included in the list of the adjustable parameters and a more detailed analysis was performed simultaneously for all the available light curves.

The final results obtained are listed in Table 5 where, for systems with mass ratio $q > 1$ the use of the reciprocal value of q (q_{inv}), as accepted in the general meaning, was used, while the obtained fits are shown in Figure 2.

Graphic representations of the systems are shown in Figure 3, using the `Binary Maker 3.0` software (Bradstreet & Steelman 2002).

TABLE 5

VALUES OF THE FIXED AND CALCULATED PARAMETERS

Parameter	J105924	J123609	J132308	J161858	J164349
Spectral type	K2 + K2	K3 + K6/K7	K4 + K6/K7	K4 + K7	K5 + K9
i	55°.028(0.129)	40°.980(0.710)	62°.070(0.392)	46°.040(0.289)	59°.368(0.055)
T_1	5022K Fixed	4860K Fixed	4480K Fixed	4580K Fixed	4380K Fixed
T_2	5018K(71)	4216K(42)	4209K(24)	4065K(18)	3909K(10)
$\Omega_{1,2}$	2.5898(0.0017)	3.9074(0.0042)	8.6765(0.0472)	2.7618(0.0039)	2.9562(0.0018)
Ω_2			9.03996 Fixed		
mass ratio q or q_{inv}	0.5017(0.0091)	0.7470(0.0261)	0.2020(0.0524)	0.5486(0.0048)	0.7499(0.0010)
ΔT	4K	644K	271K	515K	471K
f	93.30%	54.80%	6.70%	63.60%	78.90%
f_2			0%		
L_{1B}	0.2189(0.0214)	0.5601(0.0192)	0.2755(0.0076)	0.6711(0.0060)	0.2908(0.0026)
L_{1V}	0.2227(0.0186)	0.5283(0.0172)	0.2623(0.0060)	0.6510(0.0054)	0.2802(0.0024)
L_{1R}	0.2233(0.01869	0.5083(0.0153)	0.2509(0.0048)	0.6411(0.0050)	0.2674(0.0021)
L_{1I}	0.2225(0.0175)	0.4909(0.0136)	0.2453(0.0039)	0.6286(0.0045)	0.2405(0.0018)
L_{2B}	0.1304(0.0099)	0.2423(0.0101)	0.6060(0.0020)	0.1664(0.0008)	0.0976(0.0010)
L_{2V}	0.1327(0.0092)	0.2807(0.0081)	0.6304(0.0018)	0.1910(0.0009)	0.1107(0.0008)
L_{2R}	0.1331(0.0088)	0.3185(0.0085)	0.6484(0.0027)	0.2162(0.0011)	0.1211(0.0011)
L_{2I}	0.1329(0.0086)	0.3525(0.0094)	0.6726(0.0031)	0.2375(0.0008)	0.1218(0.0012)
L_{3B}	0.5809(0.0193)	0	0	0	0.5485(0.0003)
L_{3V}	0.5755(0.0189)	0	0	0	0.5510(0.0003)
L_{3R}	0.5844(0.0186)	0	0	0	0.5556(0.0005)
L_{3I}	0.5914(0.0182)	0	0	0	0.5844(0.0004)
R_{1pole}	0.4679(0.0018)	0.3745(0.0035)	0.2572(0.0043)	0.4421(0.0011)	0.4408(0.0002)
R_{1side}	0.5134(0.0030)	0.4008(0.0049)	0.2712(0.0053)	0.4780(0.0016)	0.4817(0.0003)
R_{1back}	0.5760(0.0069)	0.4679(0.0123)	0.3339(0.0157)	0.5255(0.0030)	0.5635(0.0008)
R_{2pole}	0.3575(0.0041)	0.4192(0.0026)	0.4856(0.0008)	0.3436(0.0019)	0.3948(0.0002)
R_{2side}	0.3859(0.0060)	0.4516(0.0039)	0.5278(0.0010)	0.3659(0.0025)	0.4286(0.0003)
R_{2back}	0.5240(0.0520)	0.5078(0.0082)	0.5505(0.0010)	0.4342(0.0067)	0.5436(0.0017)
Σ	0.00075351	0.00237069	0.00207468	0.00155913	0.00058782
Lat_{spot}		89°.4(0.9)	41°.7(1.2)	121°(1.9)	99°.5(1.7)
$Long_{spot}$		110°.6(1.3)	285°.2(1.9)	79°.2(1.4)	85°.2(1.2)
Radius		28°.7(0.56)	35°.5(0.89)	36°.7(0.63)	48°.5(1.11)
T/F		1.035(0.04)	0.945(0.08)	0.750(0.08)	1.03(0.06)
Component		1	2	1	1

5. EVOLUTIONARY STATUS OF THE SYSTEMS

For the determination of the absolute parameters of the systems under study, we used the relationship $P - a$ (period–semi-major axis) developed by Dimitrov & Kjurkchieva (2015). This relationship was developed based on 14 binary stars having $P < 0.27$d as follows:

$$a = -1.154 + 14.633\,P - 10.319\,P^2 \qquad (4)$$

where P is given in days and a in solar radii.

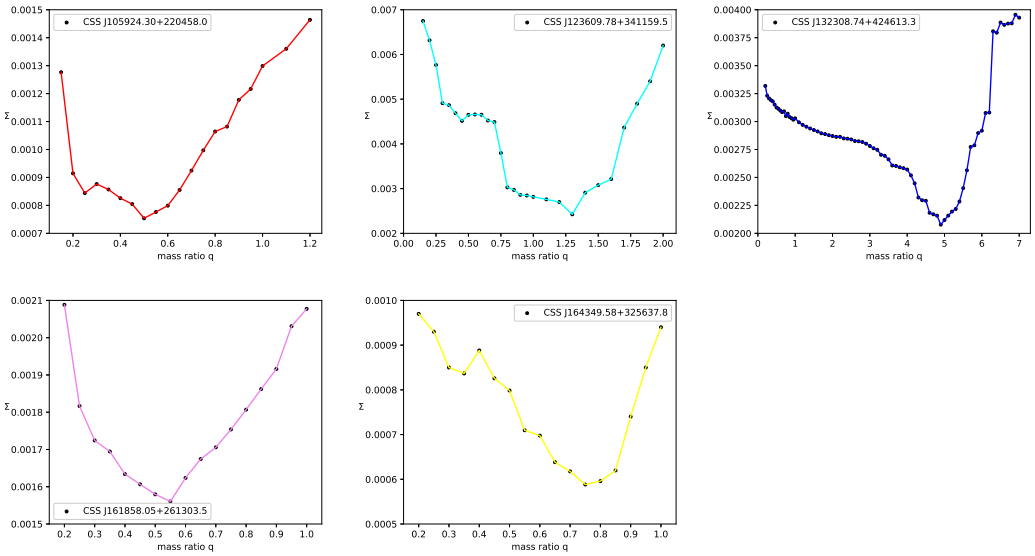

Fig. 1. The relation Σ (the mean residuals for input data) versus mass-ratio q. The color figure can be viewed online.

TABLE 6

ESTIMATED ABSOLUTE ELEMENTS

Target	J105924	J123609	J132308	J161858	J164349
Sub-type	A	W	Semidetached	A	A
$L_{1\odot}$	0.423(0.033)	0.361(0.024)	0.201(0.017)	0.252(0.021)	0.212(0.013)
$L_{2\odot}$	0.280(0.035)	0.166(0.019)	0.078(0.009)	0.098(0.011)	0.114(0.008)
$R_{1\odot}$	0.860(0.033)	0.848(0.028)	0.843(0.025)	0.797(0.027)	0.801(0.025)
$R_{2\odot}$	0.700(0.030)	0.764(0.029)	0.464(0.025)	0.630(0.030)	0.737(0.024)
a	1.65(0.05)	1.84(0.05)	1.61(0.05)	1.65(0.05)	1.61(0.05)
$M_{1\odot}$	0.773(0.078)	0.780(0.050)	0.931(0.077)	0.748(0.073)	0.639(0.058)
$M_{2\odot}$	0.388(0.046)	0.582(0.096)	0.188(0.020)	0.410(0.044)	0.479(0.044)
$\log_{g1}$	4.40	4.41	4.50	4.45	4.38
$\log_{g2}$	4.28	4.38	4.32	4.39	4.33
J_0	2.15^{51}	3.19^{51}	1.27^{51}	2.21^{51}	2.22^{51}
$\log J_0$	51.34	51.50	51.10	51.35	51.35
J_{lim}	2.66^{51}	3.53^{51}	2.50^{51}	2.65^{51}	2.49^{51}
$\log J_{lim}$	51.42	51.55	51.40	51.42	51.40

Knowing the semi-major axis a the total mass was determined and, with the fractional radii of the systems $r_{1,2}$, we calculated the absolute radii $R_{1,2}$ and therefore the absolute luminosities $L_{1,2}$.

Finally, following Wilson (1978), we may make a comparison between the absolute separation a_k from Kepler's law:

$$a_k = 4.2088\, P^{2/3}\,(1+q)^{1/3}\, M_1^{1/3} \qquad (5)$$

and the separation that the system would have in contact a_z

$$a_z = (1+q)^{0.6}\,\frac{M_1^{0.61}}{r_h + r_g}\,. \qquad (6)$$

For the value of M_1 as given in Table 6 all the systems turns out to be not a zero-age contact systems, because we have always $a_k > a_z$.

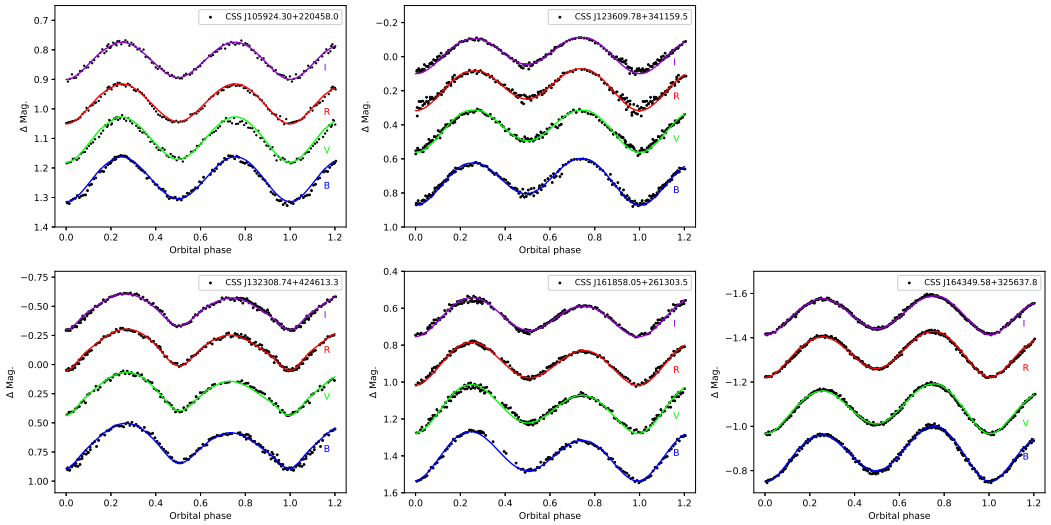

Fig. 2. CCD light curves of the systems. The points are the original CCD observations and the full lines are the theoretical fits with the surface spot contribution and third light. The color figure can be viewed online.

To investigate the current evolutionary status of our systems, the physical parameters listed in Table 6 are used.

In Figure 4, we plotted the primary, more massive (circles) and secondary, less massive (diamonds) components together with other W- and A-type W UMa systems collected by Latković et al. (2021) in the logarithmic mass-luminosity ($M-L$) relations along with the ZAMS and TAMS computed by Girardi et al. (2000).

As it is clear from the Figure 4, both components of the systems seem to be in good agreement with the well-known W UMa binaries on the $\log M - \log L$ plane. The location of the primary components is between the ZAMS and TAMS lines; that means that they are slightly evolved. Only the primary component of J132308 is located under the ZAMS as an unevolved star.

On the other hand, the secondary components deviate significantly from ZAMS like most of the secondaries of other W UMa systems.

Also, the secondary component of J132308 is located far from the other secondaries, overluminous and oversized with respect to its present mass.

For all the systems we calculated the orbital angular momentum J_0 (Eker et al. 2006) and its position in the logarithmic $J_0 - M$ diagram (Figure 5). The value of $\log J_0$ as reported in Table 6, indicates that the systems are beyond the curved limit (separating the detached and contact systems) in the region of contact.

The physical significance of this limit is that it marks the maximum orbital angular momentum (OAM) for a contact system to survive. If the OAM of a contact system is more than J_{lim} , the contact configuration breaks.

Our semi-detached system J132308 is located in the contact region endorsing the hypothesis that the system is only formally semi-detached, and we can consider it as a contact system at a key turn-off as predicted by the TRO theory.

Finally, following the work of Qian et al. (2020), who investigated the period-temperature relation of contact binary systems using the LAMOST stellar atmospheric parameters, and constructed the heat map for this relation as shown in our Figure 6, we can see that our systems are located inside the red and blue lines that are the boundaries of the normal EW systems.

The position of J132308 suggests again that it could be a system at the beginning of the contact phase.

6. DETAILS OF THE SYSTEMS AND FINAL REMARKS

6.1. *Common Features*

6.1.1. *Short Period*

Our systems possess a short period, four with $P \in (0.225, 0.229)$d and one with $P = 0.248$d.

It is known that W UMa-type eclipsing binaries show a period cut-off around 0.22 day (Ruciński (1992); Ruciński (2007)). Despite several theories

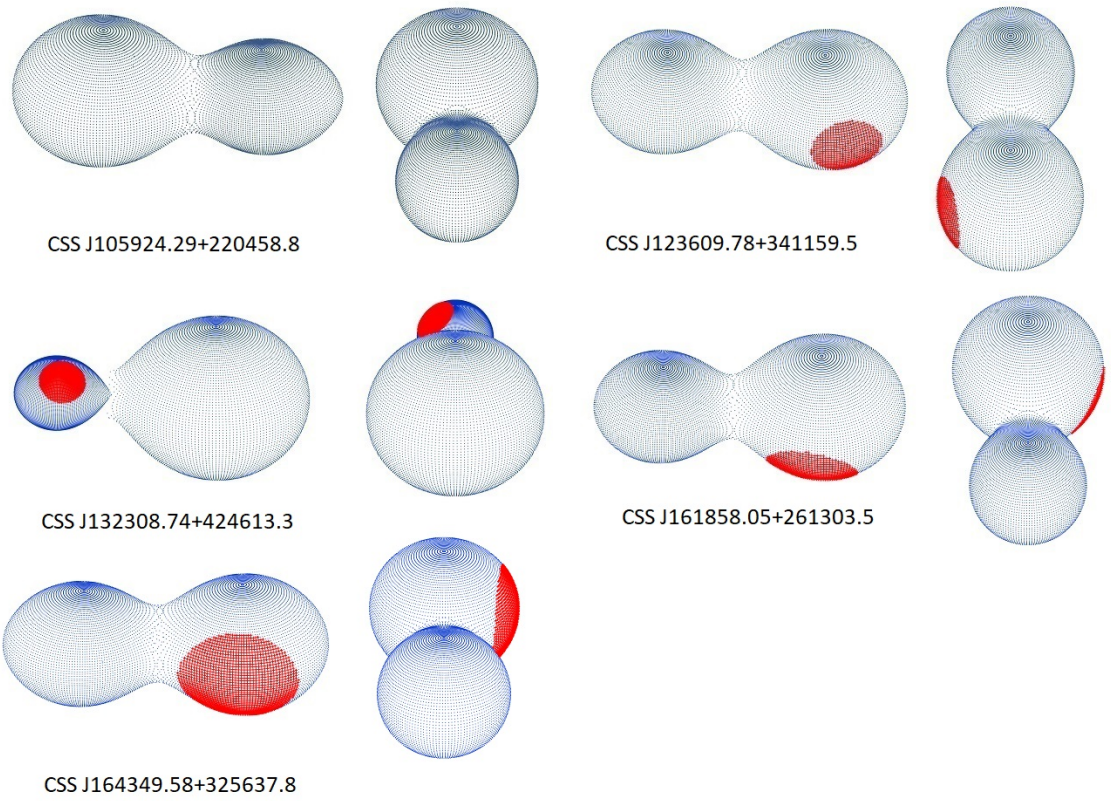

Fig. 3. Graphic images of the systems at quadrature (left) and at the primary minimum (right) according to our solution. The color figure can be viewed online.

(Stępień 2006; Jiang et al. 2012; Li et al. 2019) tried to explain this abrupt short period limit, the question is still open.

Thanks to the increase of survey missions newer EWs were found in the last years, so that it was possible to fix now this limit at the new value of $P \approx 0.15$ day determined by Zhang & Qian (2020); Qian et al. (2020); however, the 0.22-day period cut-off remains (Li et al. 2019).

The systems near the short-period end, according to the period–color relation for contact binaries, are expected to be composed of two K or later-type components (Zhu et al. 2015) with short periods ($P < 0.3$d) and to be very close to the short period limit.

6.1.2. *K Spectral Type*

K-type contact systems are rare objects and of great interest to investigate the cause of the period cut-off, and to study the structure and evolution of eclipsing binaries (TRO theory).

It is expected that K-type contact binaries, due to the presence of deep convective envelopes and fast rotation, would present magnetic activity, and dark/hot spots should be observed on one or both of the components.

Both components of the five systems studied here belong to the K spectral type and four are found to be spotted.

6.1.3. *Low Inclination*

The low inclination, between 41° and 62°, is another common characteristic of the systems here presented; values like this are often seen in other contact binaries.

Without spectroscopic data available, the W-D solution may not give the correct solution for such partially eclipsing binaries and hence the corresponding results are preliminary solutions to unveil the nature of the variables. To improve the determination of the mass ratios we applied the q-search procedure.

6.1.4. *Low Mass Contact Binaries*

Except for J123609, the other four systems possess the typical characteristics of the low mass contact binaries (LMCBs) as proposed by Stępień& Gazeas (2012), that is, systems where the total mass is under $1.0 - 1.2 M_{\odot}$.

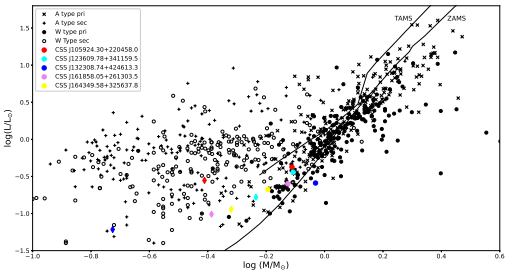

Fig. 4. Location of the components of our systems on the $\log M - \log L$ diagram. The primaries are marked with circles and the secondaries with diamonds. The sample of W UMa type systems was obtained from a compilation of Latković et al. (2021). zero age main sequence (ZAMS) and terminal age main sequence (TAMS) are taken from Girardi et al. (2000) for the solar chemical composition. The color figure can be viewed online.

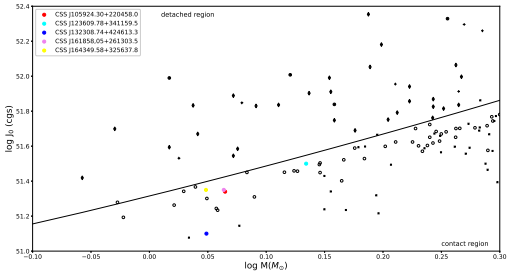

Fig. 5. The position of the five systems in the $\log J_0 - \log M$ diagram is under the J_{lim} borderline, which justifies the geometrical contact situation. The color figure can be viewed online.

6.2. *CSS J105924.29+220458.8 and CSS J161858.05+261303*

J105924 and J161858 are short period ($P \approx 0.23$d) A sub-type systems with an unusual mass ratio ($q = 0.5 - 0.55$), in relation to its overcontact factor ($f \approx 93.3\%$ and $f \approx 63.6\%$ respectively); the former is in thermal equilibrium ($\Delta T = 4$K), while the latter is not ($\Delta T = 515$K).

Generally, deep, low mass ratio contact binaries (DLMR) have high fill-out factors ($f > 50\%$) and mass ratios q less than 0.25 (Qian et al. 2006). It is believed that they could be pre-merger systems, progenitors of single rapid rotating stars as FK comtype stars, blue straggler and luminous red novae such as V1309 Sco (Stępień (2011); Tylenda et al. (2011); Zhu et al. (2016); Liao et al. (2017)).

The existence of a value of the mass ratio q_{min}, defined as the value of q under which a binary system quickly merges into a single rapidly rotating star, was investigated by many authors. Its value ranges

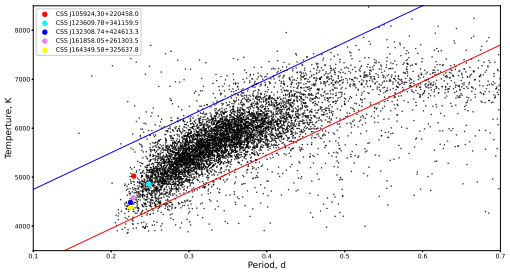

Fig. 6. Correlation between orbital period and temperature based on parameters of 8510 contact binaries from Qian et al. (2020). The red and blue lines are the boundaries of normal EWs. The color figure can be viewed online.

from $q_{min} \approx 0.109$ (Arbutina 2007) to $q_{min} \approx 0.044$ (Yang & Qian 2015).

J105429 and J161858 seem to be in contradiction, but they are not alone, other targets were found with those characteristics and they are summarized in Table 7.

From Table 7 is easy to see that among the nine systems, eight belong to the subtype A of the W UMa group, all have late spectral types (from K to M), for four of them a third light was found during the analysis of the light curves, for another one the third light cannot be excluded, while for four the third light has not a relevant value.

The presence of a third body is, according to different authors, one of most probable causes of this contradiction. In fact, it justifies the deep fill-out factor, and the angular momentum loss (AML) extracted by the stellar companion can be the cause of this rapid orbit shrinking (Stępień (2006); Stępień (2011)).

The light curves of J105924 are symmetrical and no significant evidence of inhomogeneities on the surfaces of the two components, i.e. the O'Connell effect, is noticeable. On the contrary, to obtain a good fit of its light curves it was necessary to invoke a cool spot on the primary component of J161858.

Li et al. (2020) analyzed the 2018 observations of J161858 done at the Ningbo Bureau of Education and Xinjiang Observatory Telescope and obtained values of the parameters sometimes similar to ours (the mass ratio, the inclination, the fractional radii) and sometimes very different.

The main differences are T_2, T_1, the presence of a third light, the low fill-out value (3.8%, Li et al. (2020), 63.6% here), the presence of a hot spot on the secondary component, while our analysis returns a cold spot on the primary component. The absolute

TABLE 7

CHARACTERISTICS OF SOME OVERCONTACT SYSTEMS WITH HIGH FILL-OUT AND HIGH MASS RATIO Q

Target	Period(days)	mass ratio	fill-out(%)	Sub-type	Spectral type	delta T(K)	3d light	Source
NSVS 925605	0.217629	0.678	70.2	A	M + M	678	Yes	[1]
1SWASP J161858.05+261303.5	0.2287771	0.549	63.6	A	K5 + K7	515	No	[2]
1SWASP J200059.78+054408.9	0.20569054	0.535	58.4	A	K3 + K4	272	not excluded	[3]
ER Cep	0.28573901	0.45	62	A	K0 + K2	232K	No	[4]
GSC 1387-0475	0.21781128	0.474	76.3	A	K3 + K4	166	Yes	[5]
EQ Cep	0.30696328	0.526	62.1	A	K2 + K3	111	No	[6]
1SWASP J075102.16+342405.3	0.20917273	0.78	95.4 - 98. 4	A	M3.5 + M4	76 - 83	Yes	[7]
1SWASP J105924.29+220458.8	0.229062	0.502	93.3	A	K2+K2	4K	Yes	[8]
OGLE-BLG-ECL 000104	0.2007504	0.42	80	W	K3+K3	-6K	No	[9]

[1] Dimitrov & Kjurkchieva (2015), [2] this paper, [3] Liu et al. (2018), [4]Liu et al. (2011), [5]Yang et al. (2010), [6]Liu et al. (2011), [7] Jiang et al. (2015), [8] This paper, [9] Papageorgiou et al. (2023).

estimated parameters, except for the value of the radius of the primary component, are comparable.

The sometimes strong differences in the parameters that come out of the W-D analysis can be surely justified by the low inclination of the system. It is well established that low inclination values can bring a W-D solution that may not give the correct solution for partially eclipsing binaries (Ruciński 2001). Moreover, the low inclination of the system influences also the correct determination of the spot parameters; the appearance (or disappearance) of a spot on one component of the system could even produce minimum depths reversal and thus the classification of the system could fluctuate between the A and W subtype, or vice versa, a classification as observed in several overcontact binary systems.

For J161858 we have calculated an orbital period decrease of $\mathrm{d}P/\mathrm{dt} = -3.21 \times 10^{-7}\mathrm{day\,yr^{-1}} = -0.028\mathrm{sec\,yr^{-1}}$. Such a variation can be explained by either mass transfer from the more massive to the secondary star or by angular momentum loss (AML) due to a magnetic stellar wind. If the parabolic variation is produced by conservative mass transfer, the transfer rate is $\mathrm{d}M_1/\mathrm{dt} = -4.25\times10^{-7}\mathrm{Myr^{-1}}$ (Kwee 1958).

Another possible mechanism for the parabolic variation is the AML is caused by magnetic braking. Guinan & Bradstreet (1988) derived an approximate formula for the period decrease rate due to spin-orbit-coupled AML of binary systems as follows:

$$\begin{aligned} \mathrm{d}P/\mathrm{dt} &= -1.1 \times 10^{-8} q^{-1}(1+q)^2(M_1+M_2)^{-5/3} \\ &\quad k_2(M_1R_2^4 + M_2R_1^4)\,P^{-7/3} \end{aligned} \tag{7}$$

where k_2 is the gyration constant. With $k_2 = 0.1$ (see Webbink (1976)), and with the absolute dimensions of Table 6 we computed the AML rate to be

$$\left(\frac{\mathrm{d}P}{\mathrm{dt}}\right)_{AML} = -4.31 \times 10^{-8}\ \mathrm{day\,yr^{-1}} \tag{8}$$

which is too small in comparison to the observed value. Therefore, with AML alone it is difficult to fully explain the observed secular period decrease.

For J161858 spectroscopic radial velocity observations are surely necessary in order to understand the configuration of the system.

6.3. *CSS J123609.78+341159.5 and CSS J164349.58+325637.8*

The principal common characteristic of these two systems is the large mass ratio ($q > 0.72$) that was first presented by Csizmadia & Klagyivik (2004).

The assumption is that in H-type contact binaries the energy transfer behavior is different than in other types of CBs, with the energy transfer rate less efficient at a given luminosity ratio.

Due to the mass ratio being close to unity, to equalize the surface temperature of the components

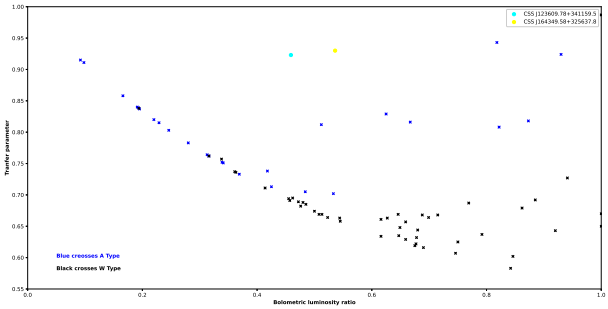

Fig. 7. Bolometric luminosity ratio λ vs transfer parameter β for J123609 and J164349. A and W-subtype are distinguished. Systems which have $q > 0.72$ are far from the position of most of the systems of the example. The color figure can be viewed online.

less luminosity should be transferred, so they have a higher transfer parameter. The transfer parameter is defined as:

$$\beta = \frac{1 + \alpha\lambda^{5.01}}{1 + \lambda} \tag{9}$$

where $\alpha = (T1/T2)^{20.01}$ and relates the temperature of the components of both the systems.

It is possible to calculate the bolometric luminosity ratio from the measured ratio in the V band via

$$\lambda = \left(\frac{L_2}{L_1}\right)_{bol} = \left(\frac{L_2}{L_1}\right)_V 10^{0.4-(BC_1-BC_2)}. \tag{10}$$

Using all the data of Csizmadia & Klagyivik (2004), in Figure 7 we plot the transfer parameter β against the bolometric luminosity ratio for our two H-systems.

Figure 7 shows that, except for the system which has $q > 0.72$, our systems have a good correlation between the bolometric luminosity ratio and the transfer parameter.

However, subsequent work by Sun et al. (2020) showed that in H-type CBs the energy transfer behavior is not significantly different from that of the remaining CBs, but the interest towards these H-type systems remains.

The secondary components of both systems are brighter and larger than their main sequence counterparts, as firstly suggested by the work of Lucy (1968), showing that the transfer of energy from the primary to the secondary is the cause of these discrepancies of luminosity and size of the secondary component.

Both systems are in physical contact with a high fill-out value, while the thermal contact is relatively far away.

The presence of third light obtained from our analysis in J164349 can explain, as for the above system J105924, the major fill-out value and the minor difference in temperature in respect to J123609 that did not show the presence of third light.

To achieve a good fit of the light curves a spot solution was considered with the result of a hot spot on the primary component of both systems.

6.4. *CSS J132308.74+424613.3*

J132308 is a semi-detached system in which the primary component is slightly greater than its Roche lobe, while the secondary component fills it.

The studies of Shaw (1994) and Zhu et al. (2010) suggest that semi-detached binaries could be in the stage between a detached binary and a contact one.

The good thermal contact between the components (ΔT=271 K), the low mass ratio ($q = 0.202$), the positive fill-out of the primary component ($f = 6.7\%$) and the shape of the light curves, that resemble those of contact binaries, suggest that this is a system in evolution toward a state of full geometrical and thermal contact.

A cool spot on the secondary component was necessary to better fit the light curves.

The star is clearly worthy of further investigation given its short period and its late spectral type.

This work is based upon observations carried out at the Observatorio Astronómico Nacional on the Sierra de San Pedro Mártir (OAN-SPM), Baja California, México. This work has made use of data from the European Space Agency (ESA) mission Gaia[5] and processed by the Gaia Data Processing and Analysis Consortium (DPAC)[6] Use of the International Variable Star Index (VSX) database has been made (operated at AAVSO Cambridge, Massachusetts, USA), as well as of the AAVSO Photometric All-Sky Survey (APASS) funded by the Robert Martin Ayers Sciences Fund. Also, use has been made of the VizieR catalogue access tool, CDS, Strasbourg, France. The original description of the VizieR service was published in A&AS 143, 23. We would like to thank the anonymous referee for her/his useful comments which improved the quality of this paper, and for calling our attention to the TESS data.

[5] https://www.cosmos.esa.int/gaia.

[6] https://www.cosmos.esa.int/web/gaia/dpac/consortium.

REFERENCES

Akerlof, C., Amrose, S., Balsano, R., et al. 2000, AJ, 119, 1901, https://doi.org/10.1086/301321

Anders, F., Khalatyan, A., Queiroz, A. B. A., et al. 2022, A&Ap, 658, 91, https://doi.org/10.1051/0004-6361/202142369

Arbutina, B. 2007, MNRAS, 377, 1635, https://doi.org/10.1111/j.1365-2966.2007.11723.x

Bai, Y., Liu, J., Bai, Z., et al. 2019, VizieR Online Data Catalog, J/AJ/158/93

Bradstreet, D. H. & Steelman, D. P. 2002, A&AS, 201, 7502

Butters, O. W., West, R. G., Anderson, D. R., et al. 2010, A&Ap, 520, 10, https://doi.org/10.1051/0004-6361/201015655

Csizmadia, S. & Klagyivik, P. 2004, A&Ap, 426, 1001, https://doi.org/10.1051/0004-6361:20040430

Dimitrov, D. P. & Kjurkchieva, D. P. 2015, MNRAS, 448, 2890, https://doi.org/10.1093/mnras/stv147

Drake, A. J., Graham, M. J., Djorgovski, S. G., et al. 2014, ApJS, 213, 9, https://doi.org/10.1088/0067-0049/213/1/9

Eker, Z., Demircan, O., Bilir, S., et al. 2006, MNRAS, 373, 1483, https://doi.org/10.1111/j.1365-2966.2006.11073.x

Flannery, B. P. 1976, ApJ, 205, 217, https://doi.org/10.1086/154266

Gaia Collaboration, Brown, A. G. A., Vallenari, A., et al. 2018, A&Ap, 616, 1, https://doi.org/10.1051/0004-6361/201833051

Girardi, L., Bressan, A., Bertelli, G., et al. 2000, A&AS, 141, 371, https://doi.org/10.1051/aas:2000126

Guinan, E. F. & Bradstreet, D. H. 1988, Formation and Evolution of Low Mass Stars, 241, 345, https://doi.org/10.1007/978-94-009-3037-7_23

Jiang, D., Han, Z., Ge, H., et al. 2012, MNRAS, 421, 2769, https://doi.org/10.1111/j.1365-2966.2011.20323.x

Jiang, L., Qian, S.-B., Zhang, J., et al. 2015, PASJ, 67, 118, https://doi.org/10.1093/pasj/psv092

Kwee, K. K. 1958, Bull. Astron. Inst. Netherlands, 14, 131

Latković, O., Čeki, A., & Lazarević, S. 2021, ApJS, 254, 10, https://doi.org/10.3847/1538-4365/abeb23

Leung, K.-C. & Wilson, R. E. 1977, ApJ, 211, 853, https://doi.org/10.1086/154994

Li, L., Zhang, F., Han, Z., et al. 2008, MNRAS, 387, 97, https://doi.org/10.1111/j.1365-2966.2008.12736.x

Li, K., Xia, Q.-Q., Michel, R., et al. 2019, MNRAS, 485, 4588, https://doi.org/10.1093/mnras/stz715

Li, K., Kim, C.-H., Xia, Q.-Q., et al. 2020, AJ, 159, 189, https://doi.org/10.3847/1538-3881/ab7cda

Li, K., Xia, Q.-Q., Kim, C.-H., et al. 2021, ApJ, 922, 122, https://doi.org/10.3847/1538-4357/ac242f

Li, K., Gao, X., Liu, X.-Y., et al. 2022, AJ, 164, 202, https://doi.org/10.3847/1538-3881/ac8ff2

Liao, W.-P., Qian, S.-B., Soonthornthum, B., et al. 2017, PASP, 129, 124204, https://doi.org/10.1088/1538-3873/aa8ded

Liu, L., Qian, S.-B., Zhu, L.-Y., et al. 2011, MNRAS, 415, 3006, https://doi.org/10.1111/j.1365-2966.2011.18914.x

Liu, N.-P., Qian, S.-B., Soonthornthum, B., et al. 2014, AJ, 147, 41, https://doi.org/10.1088/0004-6256/147/2/41

Liu, L., Qian, S.-B., Fernández Lajús, E., et al. 2018, Ap&SS, 363, 15, https://doi.org/10.1007/s10509-017-3227-4

Lohr, M. E., Norton, A. J., Kolb, U. C., et al. 2013, A&Ap, 549, 86, https://doi.org/10.1051/0004-6361/201220562

Lucy, L. B. 1967, ZAp, 65, 89

_____. 1968, ApJ, 151, 1123, https://doi.org/10.1086/149510

_____. 1976, ApJ, 205, 208, https://doi.org/10.1086/154265

Marsh, F. M., Prince, T. A., Mahabal, A. A., et al. 2017, MNRAS, 465, 4678, https://doi.org/10.1093/mnras/stw2110

Miller, A. A. 2015, ApJ, 811, 30, https://doi.org/10.1088/0004-637X/811/1/30

O'Connell, D. J. K. 1951, PRCO, 2, 85

Paczyński, B., Szczygieł, D. M., Pilecki, B., et al. 2006, MNRAS, 368, 1311, https://doi.org/10.1111/j.1365-2966.2006.10223.x

Paegert, M., Stassun, K. G., Collins, K. A., et al. 2021, arXiv:2108.04778, https://doi.org/10.48550/arXiv.2108.04778

Papageorgiou, A., Christopoulou, P.-E., Ferreira Lopes, C. E., et al. 2023, AJ, 165, 80, https://doi.org/10.3847/1538-3881/aca65a

Prša, A., Kochoska, A., Conroy, K. E., et al. 2022, ApJS, 258, 16, https://doi.org/10.26093/cds/vizier.22580016

Qian, S., Yang, Y., Zhu, L., et al. 2006, Ap&SS, 304, 25, https://doi.org/10.1007/s10509-006-9114-z

Qian, S.-B., Zhu, L.-Y., Liu, L., et al. 2020, Research in Astronomy and Astrophysics, 20, 163, https://doi.org/10.1088/1674-4527/20/10/163

Robertson, J. A. & Eggleton, P. P. 1977, MNRAS, 179, 359, https://doi.org/10.1093/mnras/179.3.359

Ruciński, S. M. 1973, Acta A., 23, 79

_____. 1992, AJ, 103, 960, https://doi.org/10.1086/116118

_____. 2001, AJ, 122, 1007, https://doi.org/10.1086/321153

_____. 2007, MNRAS, 382, 393, https://doi.org/10.1111/j.1365-2966.2007.12377.x

Ruciński, S. M. & Pribulla, T. 2008, MNRAS, 388, 1831, https://doi.org/10.1111/j.1365-2966.2008.13508.x

Samus', N. N., Kazarovets, E. V., Durlevich, O. V., Kireeva, N. N. & Pastukhova, E. N. 2017, ARep, 61, 80, https://doi.org/10.1134/S1063772917010085

Shaw, J. S. 1994, Mem. Soc. Astron. Italiana, 65, 95
Stassun, K. G., Oelkers, R. J., Pepper, J., et al. 2018, AJ, 156, 102, https://doi.org/10.3847/1538-3881/aad050
Stassun, K. G., Oelkers, R. J., Paegert, M., et al. 2019, AJ, 158, 138, https://doi.org/10.3847/1538-3881/ab3467
Stępień, K. 2006, Acta A., 56, 347, https://doi.org/10.48550/arXiv.astro-ph/0701529
_____. 2011, Acta A., 61, 139, https://doi.org/10.48550/arXiv.1105.2645
Stępień, K. & Gazeas, K. 2012, Acta A., 62, 153, https://doi.org/10.48550/arXiv.1207.3929
Sun, W., Chen, X., Deng, L., & de Grijs, R. 2020, ApJS, 247, 50, https://doi.org/10.3847/1538-4365/ab7894
Tonry, J. L., Denneau, L., Flewelling, H., et al. 2018, ApJ, 867, 105, https://doi.org/10.3847/1538-4357/aae386
Tylenda, R., Hajduk, M., Kamiński, T., et al. 2011, A&Ap, 528, 114, https://doi.org/10.1051/0004-6361/201016221
van Hamme, W. 1993, AJ, 106, 2096, https://doi.org/10.1086/116788
Webbink, R. F. 1976, ApJ, 209, 829, https://doi.org/10.1086/154781
Wilson, R. E. & Devinney, E. J. 1971, ApJ, 166, 605, https://doi.org/10.1086/150986
Wilson, R. E. 1978, ApJ, 224, 885, https://doi.org/10.1086/156438
_____. 1990, ApJ, 356, 613, https://doi.org/10.1086/168867
Wilson, R. E. & van Hamme, W., 2016, Computing Binary Stars Observables, <ftp.astro.ufl.edu>, directory pub/wilson/lcdc2015
Yakut, K. & Eggleton, P. P. 2005, ApJ, 629, 1055, https://doi.org/10.1086/431300
Yang, Y.-G., Wei, J.-Y., & Li, H.-L. 2010, New Astronomy, 15, 155, https://doi.org/10.1016/j.newast.2009.07.009
Yang, Y.-G. & Qian, S.-B. 2015, AJ, 150, 69, https://doi.org/10.1088/0004-6256/150/3/69
Zhang, X.-D. & Qian, S.-B. 2020, MNRAS, 497, 3493, https://doi.org/10.1093/mnras/staa2166
Zhu, L., Qian, S.-B., Mikulášek, Z., et al. 2010, AJ, 140, 215, https://doi.org/10.1088/0004-6256/140/1/215
Zhu, L.-Y., Qian, S.-B., Jiang, L.-Q., et al. 2015, Living Together: Planets, Host Stars and Binaries, ed. S. M. Ruciński, G. Torres, & M. Zejda, 496, 200
Zhu, L.-Y., Zhao, E.-G., & Zhou, X. 2016, RAA, 16, 68, https://doi.org/10.1088/1674-4527/16/4/068

F. Acerbi: Via Zoncada 51, Codogno, LO, 26845, Italy (acerbifr@tin.it).
C. Barani: Via Molinetto 35, Triulza di Codogno, LO, 26845, Italy (cvbarani@alice.it).
M. Martignoni: Via Don G. Minzoni 26/D, Magnago, MI, 20020, Italy (massimiliano.martignoni@outlook.it).
R. Michel, H. Aceves & L. Altamirano-Dévora: Instituto de Astronomia, UNAM. A.P. 106, 22800 Ensenada, BC, Mexico (rmm, aceves, lili@astro.unam.mx).
F. J. Tamayo: Facultad de Ciencias Físico-Matemáticas, UANL, 66451 San Nicolás de los Garza, NL, México (francisco.tamayomy@uanl.edu.mx).